Status of JLC Accelerators Development

Yong Ho Chin, Toshiyasu Higo, and Junji Urakawa

High Energy Accelerator Research Organization (KEK)

Abstract. In this paper, we summarize the status of the JLC X-band linac development and ATF (Accelerator Test Facility) activity. The report on the C-band RF system development can be found in Ref.1.

X-BAND MAIN LINAC

The main X-band linac consists of klystrons, modulators, DLDS pulse compression/delivery systems, and RF accelerating structures. The periodic permanent magnet (PPM) klystrons are under development in the two-year/two-stage project with Toshiba. The goal is to produce 50MW output power at 1.5 μs pulse length at the first klystron and then to advance to 75MW at the second one. The first PPM klystron has been tested since July 2000, and it outperforms its goal and all other (solenoid-focussed) X-band klystrons built at KEK. As for the modulator, the three-stage IGBT modulator module was tested successfully and produced 6kV-2kA output pulse. KEK is developing the multi-mode 2x2 DLDS (Delay Line Distribution System) power distribution system, in which the stability of linearly polarized TE_{12} mode in a long (up to 160m) waveguide is the key for low loss power transport. The experiment was carried out successfully in the ATF linac tunnel in collaboration with SLAC using a specially installed 55m long waveguide. Details of these developments and measurement results are presented.

Klystrons

The 1-TeV JLC (Japan e^+e^- Linear Collider) project [2] requires about 3200 (/linac) klystrons operating at 75 MW output power with 1.5 μs pulse length. Periodic Permanent Magnet (PPM) klystrons are being developed to eliminate the expense and power requirements of the focusing solenoids. KEK has begun a two-year project with Toshiba to produce two PPM klystrons in two stages. The design parameters of those klystrons are shown in Table 1. The main emphasis of the Toshiba PPM-1 klystron is to test a new gun design and to study the design and manufacturing of the PPM circuit. The damping structure of parasitic modes was adapted by using the stainless steel and the Monel as the tube and cavity materials and by tilting the output couplers slightly to break the symmetry in the output cavity. Figure 1 shows the Toshiba PPM-1 klystron before mounted on the test bench. The high power testing of the Toshiba PPM-1 klystron was started in July 2000 and is still under way. Figure 2 shows the output power as a function of the cathode voltage. Up to the date (November 9,2000), it achieved the maximum output power of 68MW at 514kV beam voltage (the corresponding efficiency is 47%).

No oscillation of parasitic mode was observed. The particle transmission was found to be 100% when no RF signal is applied. At the design pulse length of 1.5 μs, the output power of 56MW was achieved so far. But, this is not the limit. Further conditioning of the windows would increase the maximum output power at 1.5 μs. From the measurement of the power gain, it was found that Toshiba fabricated the two gain cavities at wrong frequencies. This results in the loss of efficiency by about 3%. The re-testing of the PPM-1 klystron is currently under way after the wrongly made cavities were corrected and more robust Kazakov windows [3] were installed.

TABLE1: Main parameters of the Toshiba PPM-1 and PPM-2 klystrons.

	Toshiba PPM-1	**Toshiba PPM-2**
Peak power (MW)	>50	75
Beam voltage (kV)	480 - 500	480 - 500
Micro-perveance	0.8	0.8
Efficiency (%)	>50	55
Pulse length (μs)	1.5	1.5
Repetition rate (pps)	50	150
Bandwidth (MHz)	80 at -1 dB	80 at -1 dB
Cooling of PPM	Air	Water

FIGURE 1: Toshiba PPM-1 klystron before mounted on the test bench.

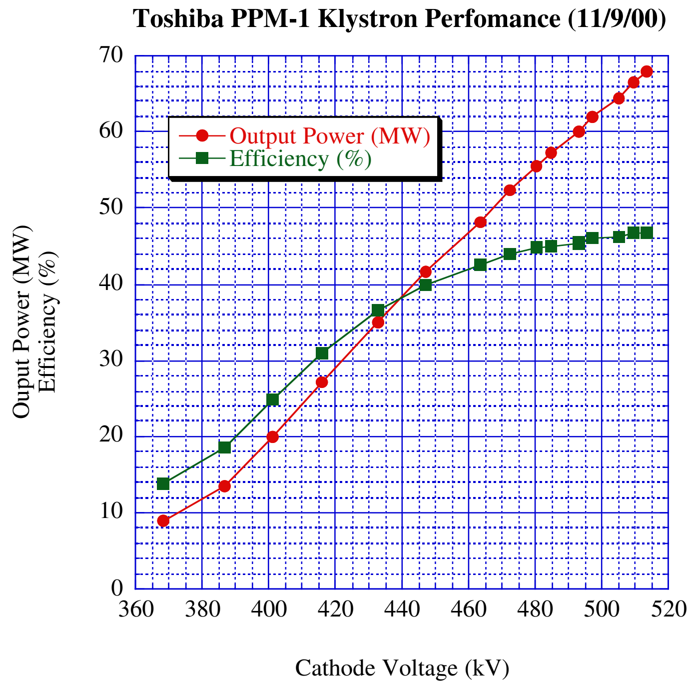

FIGURE 2: Output power vs. cathode voltage at Toshiba PPM-1 klystron

The second PPM klystron is now in manufacturing. This klystron incorporates experience and knowledge gained from the design and testing of Toshiba PPM-1. The main goals of the Toshiba PPM-2 are to manufacture a PPM klystron that meets the specifications of the JLC project and to refine the design and manufacturing process for future mass production. To meet these goals, the PPM-2 has the water-cooling to allow a higher repetition. The RF system was also improved for a higher efficiency. The high power testing is to start in April 2001.

DLDS Pulse Compression and Distribution System

In the simplest DLDS (Delay Line Distribution System), illustrated in Fig.3, the RF power from two klystrons with independent phasing is combined through a 3-dB coupler. One output port of the 3-dB hybrid is connected, through low-loss waveguide, to a linac feed about one half of the compressed pulse width times the speed of light upstream of the klystrons; the other port is connected to a local feed. The first half of the input RF pulse, of duration equal to the sum of the structure fills time and the bunch train time, is sent to the upstream feed through the delay. The second half of the RF pulse is fed into the linac close to the klystrons, without delay [4].

The largest drawback of the original (single mode) DLDS is that it requires long waveguides: a maximum of 17 waveguides run together inside the linac tunnel. A conceptual improvement was proposed by SLAC to further reduce the length of waveguide system by multiplexing several low-loss RF modes in a same waveguide. Thus, the sub-pulses in the distribution waveguide are carried by different waveguide modes so that they can be extracted at designated locations according to their mode patterns. Taking advantage of both the single mode and the multi-mode DLDS, a 2x2 DLDS was proposed at KEK to deliver RF power to four RF clusters [5]. Its scheme is illustrated in Fig.4. It consists of almost identical dual mode DLDS systems with long and short waveguide. Only two modes (TE_{01} and TE_{02} or TE_{12}) are used in each waveguide to minimize the complication caused by handling of multi-modes in one waveguide, while still providing some of the benefit of multi-mode operation by considerably reducing the total length of waveguide. The advantages of 2x2 DLDS can be summarized as (1) Cost saving: It reduces the total length of waveguide to 2/3 of single mode DLDS. (2) High efficiency: The power loss is about 30% smaller than the SLAC 3+1 DLDS. (3) High expandability: It can be easily expanded to feed up to 5-7 RF clusters. The last advantage is truly beneficial for cutting the construction cost of LC if a long RF pulse (2-3 μs) is available from klystrons in the future.

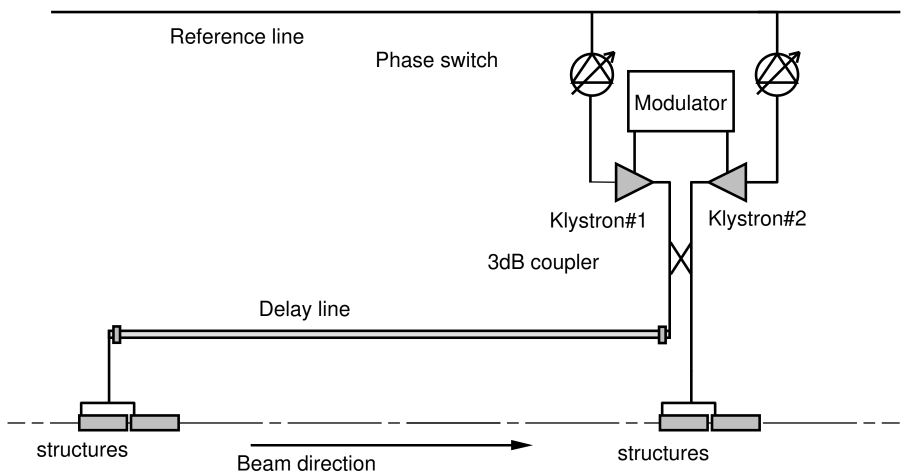

FIGURE 3: A schematic diagram of the simplest factor-2 DLDS.

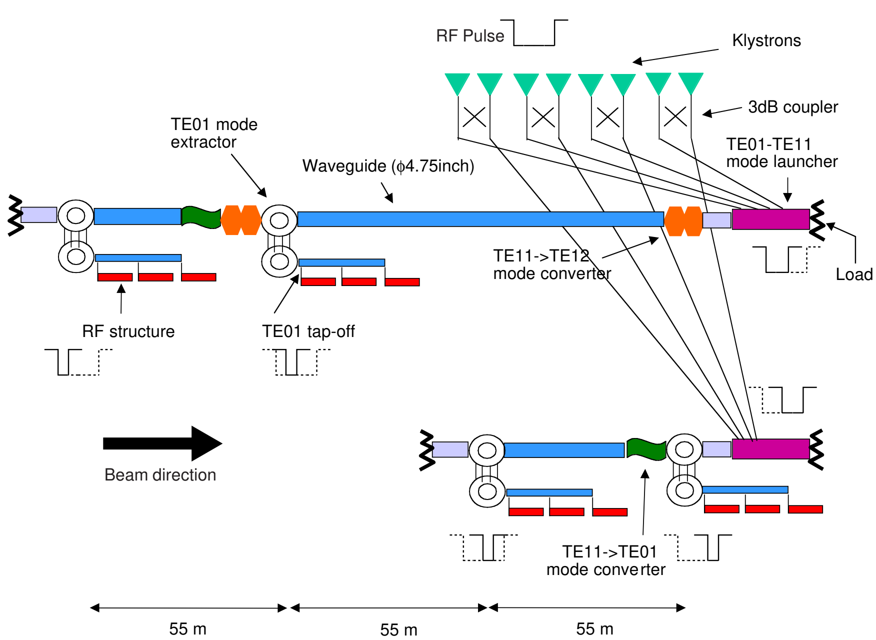

FIGURE 4: Schematic view of 2x2 DLDS.

To demonstrate the fundamental principle of the 2x2 DLDS, a cold model of the dual mode DLDS basic unit (almost identical to the system with the shorter waveguide manufactured and tested at KEK. The testing results proved that it was plausible to deliver power at different places using different modes with good efficiency (better than 95%) [4].

The critical issue in this scheme is the stability of linearly polarized TE_{12} mode in a long waveguide (that of theTE_{01} mode has been well investigated at SLED-II). Joint experiments with SLAC were performed at KEK on a delay line assembled in the ATF linac tunnel [6]. The typical setup is illustrated in Fig. 5. The transport line in our experiment was composed of eleven sections of a circular waveguide with a diameter of 12.065 cm. Each section was five meters long, for a total length of 55 meters. The sections were connected using a choked flange. This connection was designed to operate well for both the TE_{01} mode and the TE_{12} mode. The mode analyzer was installed at the end of the line to measure mode conversion due to this highly over-moded waveguide (102 modes can propagate in this guide.). The experimental findings can be summarized as follows:

1. The rotation of the TE_{12} mode is smaller than 1 degree. Furthermore, the level of the circularly polarized component in both cases is very small. Hence one can conclude that there is no significant mode cross polarization mixing.
2. The mode contamination in all modes is well below -20 dB before and after the transport line.

The overall level of the signal received is -0.37 dB, which indicates that approximately 8.5% of the input power has been lost. This cannot be accounted for by the losses in the two mode transducers and the arc-tapers (4.5%), the transmission line losses (theoretically 2.8%), plus mode conversion to theTE_{14} mode (0.5%). One can only conjecture that there are additional losses due to conversion to some TM modes, which were not measured by our mode analyzer.

From this experiment, one can conclude that the TE_{12} mode can be used as one of the dual modes in the 2x2 DLDS. Recently, the difference scheme of the 2x2 DLDS was proposed at KEK in which theTE_{02} mode is used instead of the TE_{12} mode. The TE_{02} mode has no electric field at the surface of the pipe, and thus it should be less sensitive to the imperfection of the pipe shape and the surface condition than the TE_{12} mode. This allows a looser tolerance for the pipe fabrication and the insertion of expansion joints (to absorb the thermal expansion of the pipe) without increasing the transmission loss too much. The experiment of TE_{02} mode stability and the measurement of loss in the 55 m long pipe were done recently at KEK and it shows that the TE_{02} mode is indeed quite stable and has a 30% smaller loss than the TE_{12} mode. The RF components for the TE01/TE02 dual DLDS were all designed and their cold models will be tested soon.

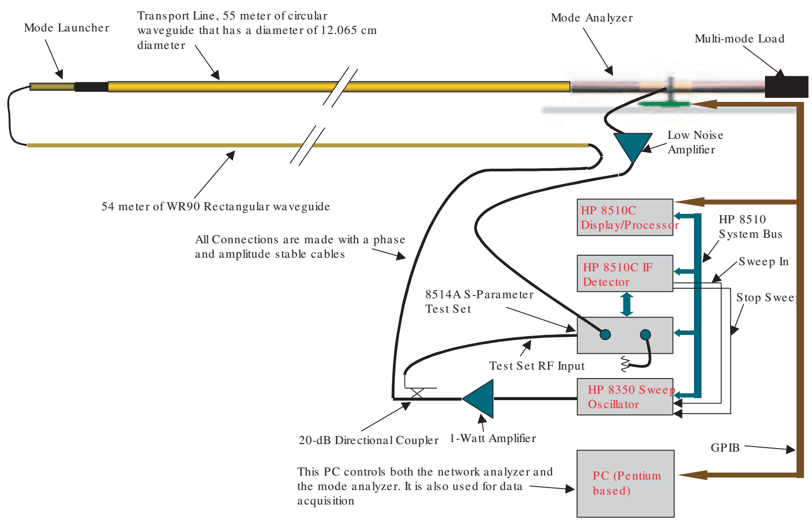

FIGURE 5: Experimental setup for TE_{12} mode transmission experiment.

Modulator

To improve the reliability of the modulator, KEK has developed a solid-state switch to replace the thyratron tubes [7]. The Static Induction SI-thyristor is suitable for the switch device because of its high-power handling and fast turn-on capability. KEK has investigated the NGK RT103N 4kV reverse conducting SI-thyristor (including freewheeling diode with press-pack ceramic housing. To evaluate the performance of this device, the fast turn-on characteristics of five stacked SI-thyristors connected in series were studied using a very low-inductance circuit. By using a coaxial structure, the residual inductance was successfully reduced to less than 136 nH. When an anode voltage of 15 kV was applied, a maximum peak current of 10 kA, dI/dt of 110 kA/μs, and switching time of 128ns were obtained. The switching time is the time required for the anode voltage to decrease to 10% of its maximum value. It was confirmed that the turn-on characteristics of the SI-thyristors are comparable to thyratrons.

Next, a 45kV solid-state switch was designed and built using the same devices. The switch uses a stack of 15 circuit card assemblies in series. Each circuit card assembly consists of a SI-thyristor, a resistor capacitor network and a gate-driving circuit. The trigger and DC power for each card were isolated from high voltage through ferrite core transformers. A photograph of the stack assembly is given in Fig. 6. The stacked devices are housed in a single cylindrical tank with a diameter of 300mm and a height of 550mm. The tank is filled with oil to insulate and cool the internal devices.

The solid-state switch performance was investigated with a line-type 5045 klystron modulator at the KEK Accelerator Test Facility, ATF. The switch was successfully operated at 45kV and 6000A with a 6μs pulse-width at 25 Hz. The switch losses were measured by calorimeter and found to be 41 J/pulse at 45kV. This value corresponds to 5% of the total PFN stored energy, with about 90% of this loss dissipated in the devices themselves. Therefore, these switches still need to be improved to further reduce losses. However, it has been confirmed that the 45 kV Si thrystor-switch has a switching capability comparable to a thyratron.

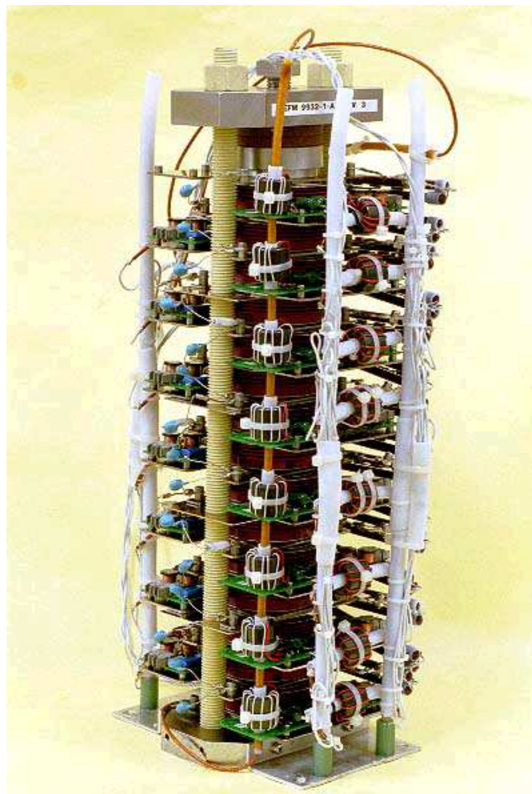

FIGURE 6: 45kV solid state switch.

KEK is now developing a new IGBT (Insulated Gate Bipolar Transistor) modulator as a two year project. The IGBT is another solid-state switch and is mainly used in trains. The IGBT typically operates at 2.5kV and switches up to 3000A. Thus, it cannot replace a thyratron as a single device and needs to be stacked. The IGBT modulator diagram is illustrated in Fig. 7. It consists of a DC power supply, four modules of switching unit at 25kV, a pulse transformer with a ratio of 1:5, and a waveform compensation circuit. Each module contains 10 stacks of energy storage capacitors, IGBT switches and IGBT gate drivers, and it produces 25kV voltage in total. The four modules are connected in a series-parallel arrangement and turns on into the primary of a pulse transformer to produce 500kV output pulse at 530A with a flat-top width of 1.5µs. A prototype of the module with only three stages for 6kV-2kA output pulse was built and tested successfully (Fig. 8). Figure 9 shows the measured voltage waveform. The waveform can be made flatter by using a waveform compensation circuit to be built in 2001.

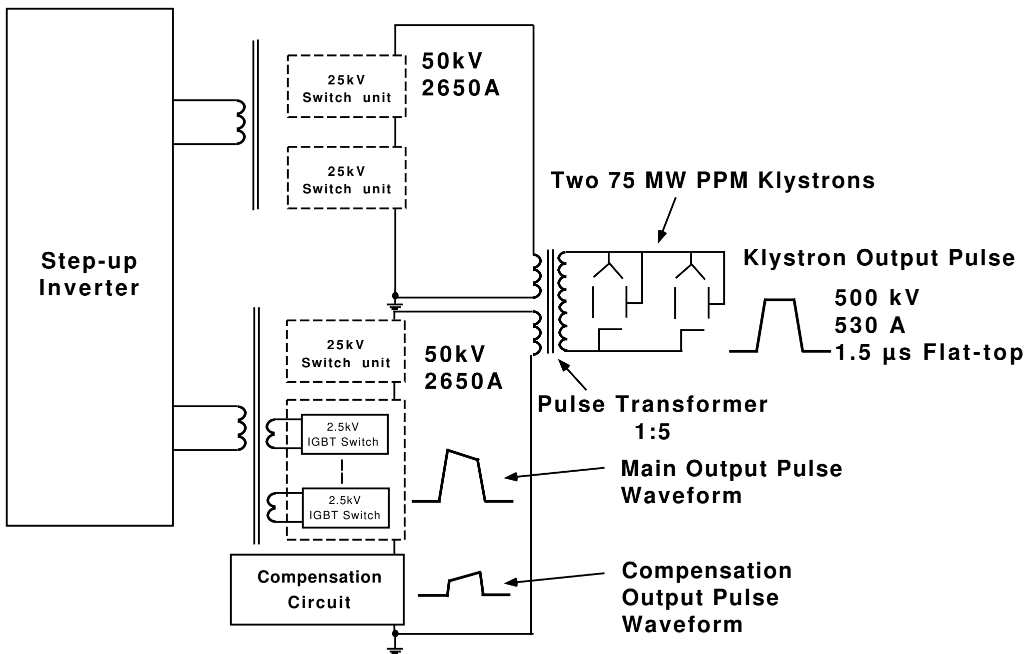

FIGURE 7: Diagram of the IGBT modulator.

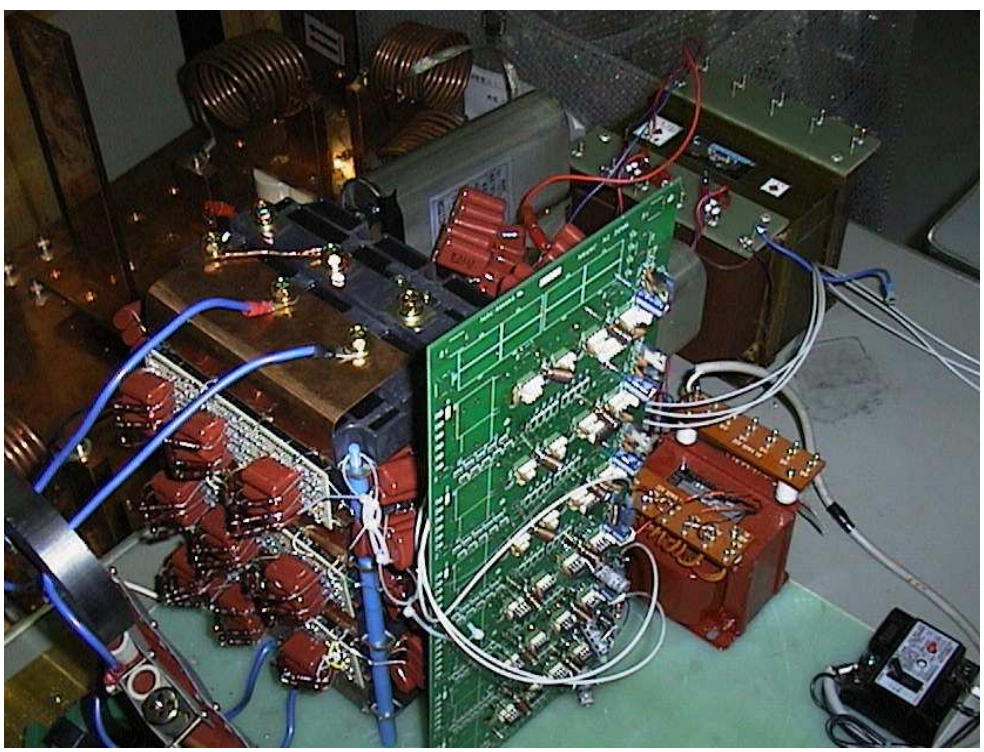

FIGURE 8: The three-stage prototype of switching module.

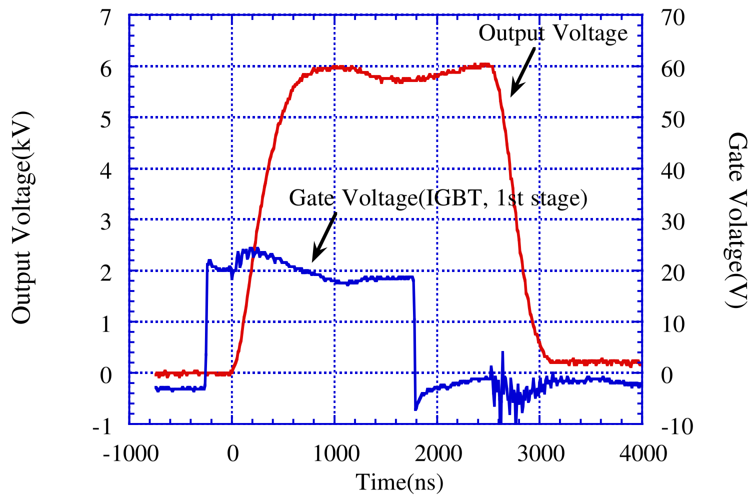

FIGURE 9: Output voltage waveform of the three-stage prototype module.

RF Structure

The required features of the main linac structures are the good alignment of the constituent cells and the realization of the design frequency distribution of the dipole modes in addition to the accelerating mode frequency tolerance [4]. These features have been realized by utilizing the present-day high-accuracy diamond turning technology followed by the diffusion bonding process. This technique has been applied in Damped Detuned Structures, DDS. Recently, a Rounded Damped Detuned Structure, RDDS, was designed to increase the shunt impedance by shaping the inner shape of each DDS accelerating cell.

In order to keep the acceleration efficiency high under random frequency errors in accelerating mode, the random error tolerance was set at 3 MHz RMS. On the other hand, we set the tolerance of 5 degrees in the integrated phase advance error at any point along the structure. This requirement is equivalent to the systematic frequency tolerance of 0.1 MHz if the error is uniform over a structure. Even though this requirement seems very tight, it can be met with applying a feed-forward in some dimension of the cells of the later fabrication during the continuous fabrication of disks.

An important requirement on the dipole-mode frequency distribution is its smoothness of its distribution. The random error in the higher-mode frequencies was 3 MHZ RMS. On the other hand, a systematic error as an offset over the whole structure does not affect the wake field at all. However, higher components of the error distributions should be within a few MHz.

We specified that the contour shape of the cell stayed within -1 μm. This amount of error limits the frequency error to be 3 MHz at maximum, even in the extremely unlucky error distribution both in the accelerating mode and in the first dipole mode. Therefore, under this tolerance, the requirement on the random error is satisfied.

The most severe requirement is the systematic frequency tolerance of the accelerating mode. If the contour shape error is within the same tolerance, the accelerating mode frequency deviates within a MHz because such dimensions as beam hole radius, "a", and accelerating cell radius, "b", are very well correlated by the help of NC characteristics so that the frequency perturbations due to "a" and "b" cancel even partly to reduce the frequency sensitivity on dimensional error considerably. In this situation with a moderate controllability of frequency, we can make a feed-forward correction to the dimension of "b" in the later fabrication of disks based on the average frequency information of the early-made disks.

Figure 10 shows the scattering of the π-mode frequencies of the dipole mode of each disk for RDDS1 structure. This frequency smoothness is essential to controlling the dipole wake field. We found that the deviation of 0.6 MHz RMS is much less than the requirement of 3 MHz.

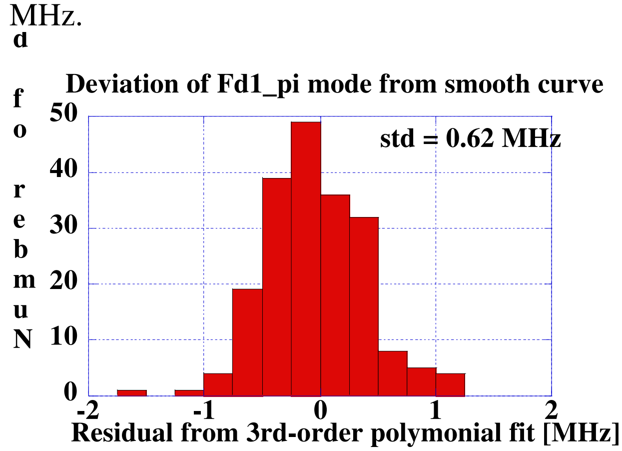

FIGURE 10: Each-disk frequency deviation from smooth fit.

In Fig. 11 are shown the measured accelerating mode frequencies, the associated integrated phase slip along the structure and the feed-forwarded values in "2b". It is seen from the figure that the integrated phase slip was kept within 5 degrees showing that the feed-forward method worked well. It is to be noted that this feed-forward mechanism can compensate not only the machining error of precision lathe but also the errors in 3D geometries made by milling machine which is usually less accurate than the precision lathe.

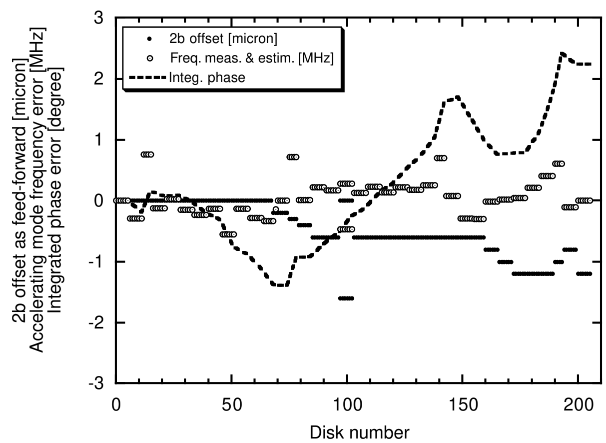

FIGURE 11: Accelerating mode frequency.

From this fabrication of the disks for the first prototype RDDS structure, we proved that the disks which satisfy the frequency requirements of both accelerating mode and dipole mode can be realized through a high-accuracy diamond turning machining with the help of a careful feed-forward technique.

ATF

The ATF [8] has been designed to investigate the feasibility of the LC operation scheme and to develop beam-control techniques for the LC. The purpose of the ATF is to develop accelerator technology that can stably supply to the main linear accelerator an extremely flat "multi-bunch beam" that can be squeezed down to a few nanometers at the collision point.

The KEK/ATF consists of an S-band high gradient linac (Linac), a beam-transport line (BT), the damping ring (DR) and an extraction line (EXT). The pre-injector was completed in Aug. '93, when the development of multi-bunch beam-diagnostics started. In Nov. '95, we completed the high-gradient linac so that experiments on the acceleration of a multi-bunch beam and on the compensation of multi-bunch beam loading could be performed. After installation of the main hardware components, in Jan. '97 we started beam commissioning in the damping ring. In November 1997, we completed the extraction line for precise beam diagnostics. Presently, we are refining the beam-tuning techniques and are stabilizing the key machine components to supply the extremely small emittance beam stably into the extraction line. Since many beam instrumentation devices in the ATF turned out not to be sufficient for precise beam tuning and measurements, we are also upgrading each of the systems and are developing new diagnostics. For example, a laser wire and skew quadrupole magnets were installed near the end of JFY '99 to measure the tiny beam size in the ring and to control the tilt of the beam at the extraction line. Table 2 summarizes the achieved accelerator performance of the ATF.

The purpose of the ATF is to generate beams with very small transverse and longitudinal emittances as required for future linear colliders. So far, a horizontal emittance of 1.4 ± 0.3 nm was measured with wire-scanners in the extraction line and with the horizontal spatial coherence using a SR interferometer. In addition, a vertical emittance of 15 ± 2.5 pm was measured with 5 wire scanners in the extraction line. Still much effort is needed in order to stably produce a beam with 10 pm vertical emittance at 1.3 GeV. A large number of beam studies conducted in the ATF Linac since JFY 1995 proved the soundness of the $\pm\Delta$F multi-bunch beam loading compensation scheme. The experiment demonstrating this scheme was conducted with 6×10^9 electrons/bunch and 20 bunches/train. The original multi-bunch energy spread of 5% from head to tail was corrected to within 0.6%. Since JFY 1994 various new instrumentation has been developed for multi-bunch high-precision beam diagnostics, for example, synchrotron and optical transition radiation (SR and OTR) monitors with 3 nsec fast gate, a micron beam size monitor using the extraction line wire scanners for emittance measurements, an SR interferometer, and a laser wire beam size monitor in the ring. All of these are still being improved in order to establish beam control techniques adequate for the micron world [9].

TABLE 2: Achieved and design parameters at ATF

Item	Achieved values	Design
ATF Linac Status		
Maximum Beam Energy	1.42GeV	& 1.54GeV
Maximum Gradient with Beam	28.7MeV/m	30MeV/m
Single Bunch Population	1.7×10^{10}	2×10^{10}
20 Multi-bunch Population	7.6×10^{10}	40×10^{10}
Bunch Spacing	2.8 ns	2.8 ns
Repetition Rate	12.5Hz	25Hz
Energy Spread (Full Width)	< 2.0% (90% beam)	<1% (90% beam)
Damping Ring Status		
Maximum Beam Energy	1.28GeV	1.54GeV
Circumference	138.6 ± 0.003m	138.6m
Momentum Compaction	0.00214	0.00214
Single Bunch Population	1.2×10^{10}	2×10^{10}
COD(peak to peak)	x≈2mm, y≈1mm	1mm
Bunch Length	≈6mm	5mm
Energy Spread	0.06%	0.08%
Horizontal Emittance	$(1.4\pm0.3) \times 10^{-9}$ m	1.4×10^{-9} m
Vertical Emittance	$(1.5\pm0.25) \times 10^{-11}$ m	1.0×10^{-11} m

ACKNOWLEDGMENTS

The authors would like to thank all members of the JLC X-band and C-band Main Linca Groups and the ATF for preparation of this document.

REFERENCES

1. H. Matsumoto, T. Shintake, et. al., "R&D status of the C-band RF-system development for e+e- Linear collider in Japan", KEK Preprint 99-83, 1999.
2. "JLC Design Report Study", KEK Report 97-1, 1997.
3. S. Y. Kazakov, KEK Report 98-120, 1998.
4. "International Study Group Progress Report on Linear Collider Development", KEK Report 2000-7, SLAC R-559, 2000.
5. J.Q. Wang, Y.H. Chin , et. al., " Study of RF Components for JLC 2x2 DLDS" in Proc. of PAC99, 1999, P.1058.
6. S. Tantawi, et. al., "Evaluation of the TE(12) Mode in Circular Waveguide for Low-Loss, High-Power RF Transmission", Phys. Rev. ST Accel. Beams 3: 082001, 2000.
7. M. Akemoto, et.al., "Development of a High-Power Klystron Modulator with SI-thyristor Switch", SSID-00-5, 2000.
8. Edited by E. Hinode, et. al., KEK Internal 95-4, 1995.
9. J. Urakawa, "Experimental results and technical research and development at ATF (KEK)", KEK Preprint 2000-67, 2000.